Progress In Electromagnetics Research C, Vol. 55, 167–177, 2014

Dual-Band Dual-Sense Unidirectional Circularly Polarized Antenna with CPW-Fed for Wireless Applications

Xiaoxiang Ding, Zhiqin Zhao*, Lin Zhou, Mubarak S. Ellis, and Zaiping Nie

Abstract—A novel dual-band unidirectional circularly polarized (CP) antenna fed by coplanar waveguide (CPW) for wireless applications is proposed. The antenna configuration consists of a ring-shaped ground, an F-shaped central strip and a spherical cap reflector. The longer and shorter branches of the F-shaped central strip help to produce radiations at lower and higher frequencies. The CP characteristics are achieved by adding two solid arcs and a grounded tuning stub. Both simulated and measured results are given and analyzed. Measurement results show a 10 dB return loss with a bandwidth of 56% (2.15 GHz–3.83 GHz) at 2.45 GHz (ISM), and a bandwidth of 42.6% (4.67 GHz–7.2 GHz) at 5.8 GHz (HiperLAN), a 3 dB axial ratio bandwidth of 15.1% (2.25 GHz–2.62 GHz), 4.1% (5.67 GHz–5.91 GHz). The maximum gains within the two CP bands are 8.7 dBic and 10.2 dBic, respectively.

1. INTRODUCTION

Due to its relative insensitivity to transmitter and receiver orientation than linearly polarized (LP) antenna, circularly polarized (CP) antenna has been widely used in wireless communication system. The most significant advantage of CP antenna over LP antenna is that it can relieve the influences of multi-path reflections caused by buildings and other obstacles. In order to enlarge the impedance bandwidth and axial ratio (AR) bandwidth, a variety of designs have been reported [1–15]. Using broadband feeding network [1–3] is an immediate and effective approach. In [2, 3], the AR bandwidth of 81.5% and 47.8% is achieved at 3 dB and 1 dB threshold respectively. However, these designs are usually complicated and they need a large ground for feeding circuits. In order to avoid these disadvantages, some single-fed broadband CP antennas [4–11] have been investigated. In [4], a microstrip antenna with about 14% 3 dB AR bandwidth is proposed. The antenna combines an U-slot and an L-probe to enhance its impedance bandwidth. Microstrip-fed and CPW-fed monopole or dipole antennas have also been widely studied for improving CP bandwidth [5–7, 10, 11]. However, these designs have relative low gains. Furthermore, the gap-coupled feed method for microstrip patch antennas [8, 9] is another way to improve AR bandwidth and impedance bandwidth. In recent years, coplanar waveguide (CPW) feed broadband CP slot antennas [12–15], whose 3 dB CP bandwidths range from 25.3% [14] to 48.8% [13], have received lots of attentions due to their merits of broadband, low profile, low cost and easy integration with monolithic microwave integrated circuits (MMIC).

The rapid development of wireless communication systems has witnessed increasing demands for multi-band antennas. Hence, some dual-band CP antennas have emerged at this moment [16–21]. Refs. [16, 17] reported some dual-band broadband CP antennas fed by microstrip lines with analogous monopole radiations and obtained 3 dB AR bandwidths of more than 15%. Other dual-band CP antennas fed by CPW can also achieve wideband characteristics by slotting an U-shaped open-slot on the ground [18], or adding a T-shaped [19] or a C-shaped [20] grounded strip with other tuning stubs

Received 15 December 2014, Accepted 15 December 2014, Scheduled 15 January 2015
* Corresponding author: Zhiqin Zhao (zqzhao@uestc.edu.cn).
The authors are with the School of Electronic Engineering, University of Electronic Science and Technology of China, Chengdu, Sichuan 611731, China.

on the central conductor. Especially in [21], a CPW-Fed slot antenna with two broad ARBWs of more than 30% is reported.

Most of these dual-band CP antennas mentioned above have bidirectional radiation patterns with low gains. In many circumstances, for instance, positioning, directional finding, point to point high-speed data communication, short range wireless local networks, etc., directional and high-gain broadband antennas are urgently needed. For the purpose of unidirectional and high-gain radiation, the most effective method is to add a metal reflector which can restrain the electromagnetic wave. Generally, there are two kinds of reflectors, the first category is reflective cavity or plate, the other category is printed metal strip [22] on a substrate. However, most unidirectional broadband CP antennas are only with a single band. A few dual-band CP antennas [23–28] with unidirectional radiation were proposed to break through this limitation. The impedance bandwidth of 19% for the upper band can be obtained due to the meandering probe feed technique [26]. A CPW-fed slot antenna with inserting a T-shaped and an L-shaped perturbation in the slot is presented and it obtains two broad CP bandwidths of more than 12% [28]. Besides that, these antennas' 10 dB impedance bandwidths are less than 8% and 3 dB AR bandwidths are no more than 3.5% [23–25, 27].

In this paper, a novel design for a CPW-fed unidirectional dual-band CP antenna with a spherical cap reflector is proposed. By using an F-shaped central strip, dual-band broadband feature can be excited, which covers the 2.45 GHz band (specified by IEEE 802.11 b/g) for ISM and the 5.8 GHz band (specified by IEEE 802.11 a) for HiperLAN. A spherical cap reflector contributing to overcome rippled and sunken pattern at the upper band compared with traditional plane reflector with the same distance is designed to realize unidirectional high gain radiation. By adjusting two solid arcs and one rectangular tuning stub embedded in the ring-shaped ground, two expected AR bandwidths are realized. The measured CP bandwidth of 15.1% at lower band and 4.1% at upper band, with peak gains as high as 8.7 dBic and 10.2 dBic in the operational bands, have been obtained.

The remainders of the paper are organized as follows. The design and analyses are presented in Section 2. Parametric analyses are given in Section 3. Section 4 provides experimental results of the fabricated antenna. Conclusions are drawn in the final section.

2. ANTENNA CONFIGURATION AND ANALYSIS

Figure 1 illustrates the structure of the proposed unidirectional dual-band dual-sense CP antenna with top view and side view. As shown in the figure, the square ring-shaped ground and F-shaped radiant

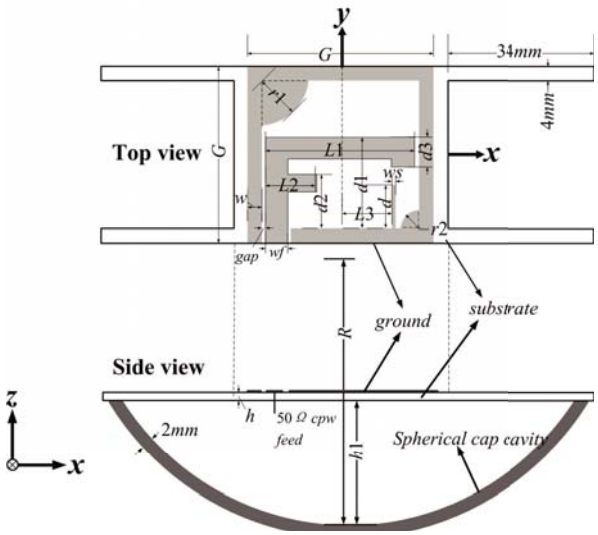

Figure 1. Geometry of the proposed antenna. ($G = 29$ mm, $w = 1.5$ mm, $L_1 = 25.5$ mm, $L_2 = 10$ mm, $L_3 = 9.25$ mm, $d = 10$ mm, $d_1 = 17$ mm, $d_2 = 9.5$ mm, $d_3 = 6$ mm, $w_s = 0.5$ mm, $w_f = 4.4$ mm, $gap = 0.3$ mm, $h = 0.8$ mm, $h_1 = 28$ mm, $R = 58$ mm, $r_1 = 8$ mm, $r_2 = 3$ mm).

central strip are printed on a microwave substrate of FR4 with a thickness of h, a relative permittivity of $\varepsilon_r = 4.4$ and a loss tangent of $\tan\delta = 0.02$. A novel spherical cap reflector of height h_1 and radius R is used to realize unidirectional high gain radiation in the two interested bands. The length of the substrate is 3 mm larger than the ring-shaped ground with a side length of G and a width of w in the horizontal right and left direction. The antenna is fed by a 50-Ω CPW transmission line, where the central strip and the two uniform gaps have a width of w_f and *gap* respectively. The lengths of the two branches of F-shaped central strip are L_1 and L_2, and the distances from branch's top to inner border of the ring-shaped ground are d_1 and d_2, respectively. At the end of the first branch, a metal trip with a length of d_3 is embedded to add antenna's electrical length at the lower band. A grounded slimsy strip with a size of $d \times w_s$ (length of d and width of w_s) is added to produce the CP wave at upper band. By optimizing the location of this strip and radii (r_1, r_2) of the two solid arcs embedded in the ground, the expected consequence will be obtained. As is shown in Figure 1, four symmetrical substrates with same thickness and a size of 34 mm × 4 mm are added for easy fabrication. The final optimal dimensions of the proposed antenna are specified at the end-note of Figure 1.

2.1. Antenna Design Process

For illuminating the design process of this proposed antenna, four prototypes are defined as shown in Figure 2. The approximate size of the ring-shaped ground is given by $\lambda_0/4 = c/4f_0$, where c is the speed of light, λ_0 is the free space wavelength of the lower band resonant frequency $f_0 = 2.45$ GHz. ANT A, as shown in Figure 2(a), is a referential antenna, which includes one long L-shaped central metal branch whose total length is 41.2 mm, corresponding to an approximation of $0.5\lambda_g$. λ_g is given by

$$\lambda_g = \frac{c}{f_0\sqrt{\varepsilon_{eff}}}, \quad \varepsilon_{eff} = \frac{\varepsilon_r + 1}{2}, \tag{1}$$

where, ε_{eff} is the approximated effective dielectric constant. As shown in Figure 2(b), ANT B has a long L-shaped central metal strip, and two solid arcs are embedded in the ground. ATN C contains a long L-shaped central metal branch, combining with a short L-shaped shunt branch, an F-shaped central radiation strip is formed (Figure 2(c)). The length of the short L-shaped strip is also designed to be about $0.5\lambda_g$, where λ_g is given by (1), but f_0 is the expectant resonant frequency (5.8 GHz) at upper band. ANT D, which is the proposed one, has a ring-shaped ground, an F-shaped central strip, and a grounded slimsy tuning strip (Figure 2(d)).

The four prototypes shown in Figure 2 have been simulated using an Ansoft commercial high frequency structure simulator (HFSS). Simulated results with return loss (RL) curve and axial ratio (AR) curve of the two operational bands are compared in Figure 3. As shown in Figure 3, ANT A with only one long L-shaped central strip has a narrow 10 dB RL bandwidth at about 2.6 GHz and a bad AR bandwidth. When two solid arcs are embedded in the ring-shaped ground, like ANT B, the impedance matching will become much better, which enlarges RL bandwidth at lower band. Meanwhile an expected 3 dB AR bandwidth is obtained as well. In Figure 3(a), ANT C can excite upper radiation band by adding a short shunt branch on the central metal strip, whereas it is only the linearly polarized (LP) wave shown in Figure 3(b). The bold solid curves shown in Figure 3 are for the proposed one (ANT D), which cover two broad bands with 10 dB RL bandwidths of 44.8% (from 2.2 GHz to 3.62 GHz)

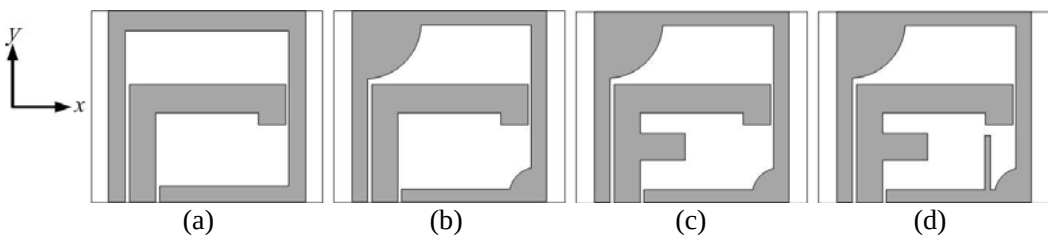

Figure 2. Evolution of the proposed antenna configuration. (a) ANT A, (b) ANT B, (c) ANT C, (d) ANT D.

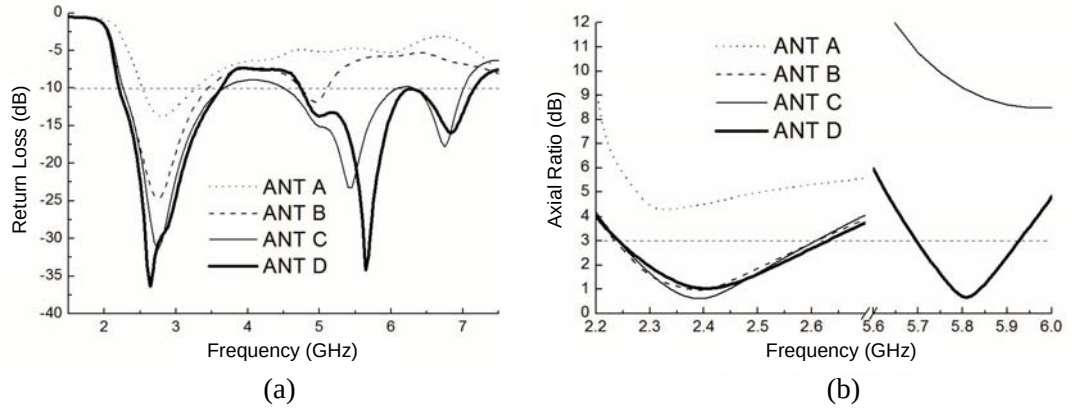

Figure 3. Simulated (a) return loss and (b) axial ratio for the four antennas shown in Figure 2.

and 40.5% (from 4.75 GHz to 7.16 GHz) including two 3 dB AR bandwidths 15.5% (from 2.24 GHz to 2.62 GHz) and 3.9% (from 5.69 GHz to 5.92 GHz), respectively.

2.2. Design of Spherical Cap Reflector

In some real applications, directional and high gain radiations are very important. An effective approach is to add a backing metal plate. Generally, due to its easy fabrication, rectangular backing plate has been widely used. According to the mirror theory, the backing plate technique prompts the antenna to become a two element array, and theoretically its gain will improve 3 dB. From the electromagnetic theory, the total electric field in the forward direction has two components, one is from the practical source, the other one is from the mirror source. It is well known that the total field becomes the strongest when the distance between the radiator and the backing reflector is $\lambda_0/4$, where λ_0 is the wavelength. However, this phenomenon just occurs at a very narrow band, its gain decreases and the sunken pattern arises out of this band. To relieve this defect and obtain a better radiation in a larger band, here we utilize a spherical cap reflector, which has a gradual structure, as shown in Figure 1. In order to validate the feasibility of this design, a traditional rectangular plate with the same width has been simulated. The distance between the radiator and the rectangular plate is also set to be 28 mm, which approximately equals to $\lambda_0/4$ at the lower frequency 2.45 GHz. Due to this fact, it can be assumed that the radiation pattern produced by the rectangular plate will just be good at the lower band, but for upper band it will be bad. The simulated radiation pattern and gain have been compared in the concerned bands with those reflectors to verify this assumption. Figure 4 and Figure 5 show that the spherical cap reflector can help to produce higher gain and better radiation patterns, especially at high frequency, e.g., 5.8 GHz.

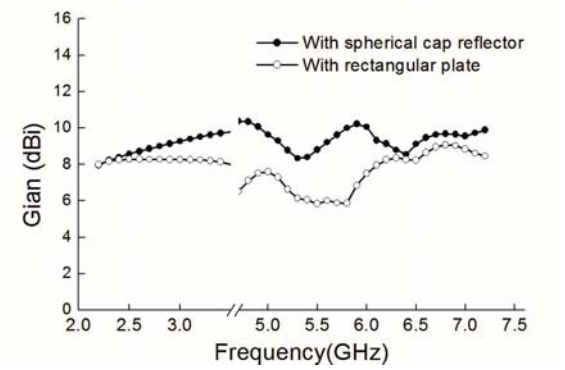

Figure 4. Simulated gains with different reflectors.

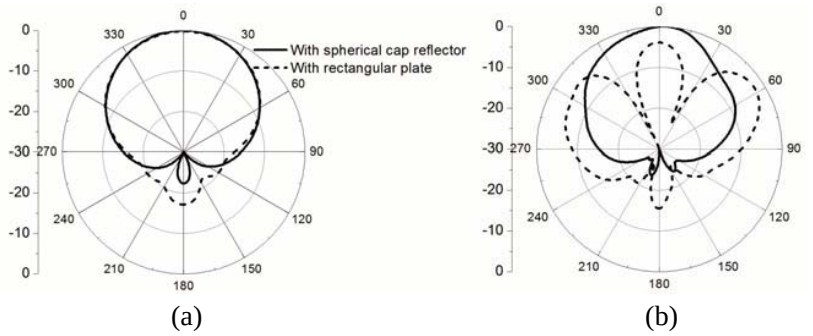

Figure 5. Simulated x-z plane radiation patterns at (a) 2.45 GHz and (b) 5.8 GHz.

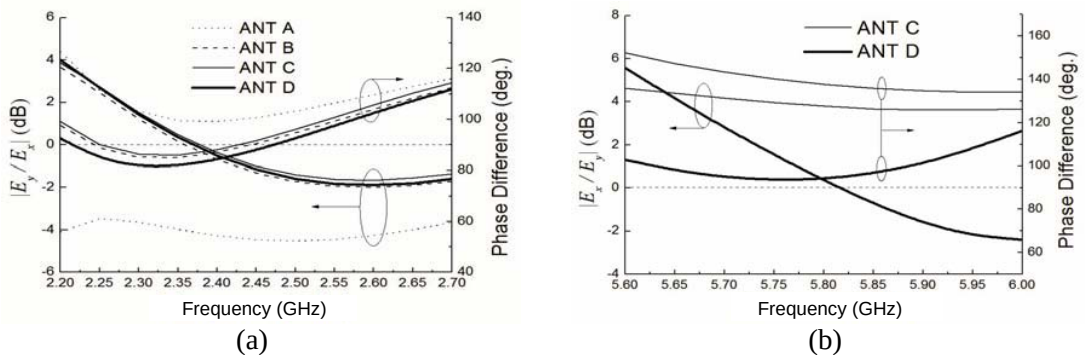

Figure 6. Simulated (a) amplitude ratio (E_y/E_x) and their PD at lower band, (b) amplitude ratio (E_x/E_y) and their PD at upper band.

2.3. Circularly Polarized Operation Principles

The inner length of the ring-shaped ground shown in Figure 2 is set to be 26 mm × 26 mm, whose structure looks like a square slot to be allowed to propagate two orthogonal components of TE_{10} and TE_{01}. Furthermore, the long horizontal and vertical branches of the F-shaped central strip in the direction of x component and y component, contribute to producing TE_{01} mode and TE_{10} mode at lower band [29], while the short ones contribute to upper band. According to the simulated port reflection coefficient, for the lower band the TE_{10} mode and the TE_{01} mode operate at 2.38 GHz and 3.05 GHz with the phase of 138.2° and 49.9°, respectively. While for the upper band, they operate at 5.28 GHz and 6.0 GHz with the phase of 152.3° and 242.4°. Circularly polarized wave is to be generated by exciting two orthogonal linearly polarized modes with an equal amplitude and a 90° phase difference (PD). In order to illustrate the CP operation of the proposed antenna, the curves of simulated amplitude ratio (dB) and phase difference (deg.) of two orthogonal far field components (E_x, E_y) in the direction of $+z$ are given in Figure 6. It is noticed that in Figure 6(a) the amplitude ratio of E_y/E_x and their PD produced by ANT A at lower band deviate from the expected values (0 dB and 90 deg.). This can be adjusted by adding a pair of grounded arcs. While the curves of ANT B, C and D have almost uniform tendencies and only slight differences around the expected values. Because in ANT B, C and D, the vertical PD is ahead of the horizontal PD at the lower band, they produce left hand circular polarization (LHCP) waves. For the higher band, the horizontal PD is ahead of the vertical PD, (as shown in Figure 6(b)), thus produces right hand circular polarization (RHCP) waves.

Surface currents are further studied to explain the LHCP and RHCP of the proposed antenna, i.e., ANT D. Figure 7 shows the currents from top side view. The surface currents in 0° and 9° phases are with equal magnitude and opposite orientation to that of 180° and 270° phases. It also can be observed that the more intensive surface currents exist on the outer ring-shaped ground at lower frequency 2.45 GHz, whereas stronger currents at higher frequency 5.8 GHz appear on the grounded tuning strip which is good for the upper band CP realization. In addition, the lower frequency currents, especially

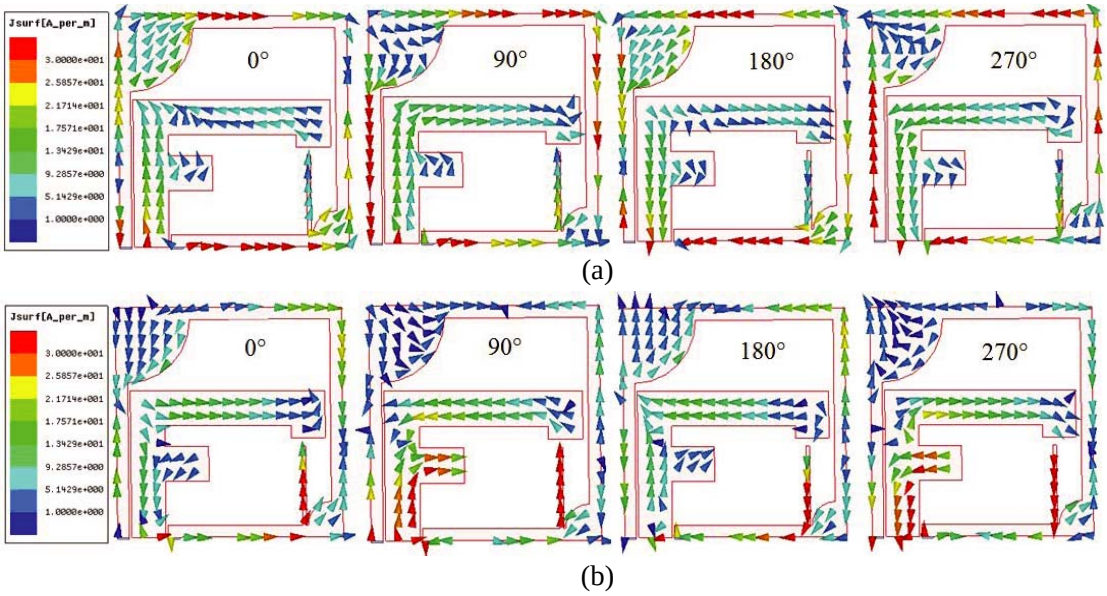

Figure 7. Simulated surface current distributions of the proposed antenna in 0°, 90°, 180° and 270° phase at (a) 2.45 GHz, (b) 5.8 GHz.

distributing on the two solid arcs and the long horizontal branch of the F-shaped central strip, perform a clockwise rotation with the changing phases, while the upper frequency currents distributed on the same two arcs and the short horizontal branch perform a anticlockwise. It is consistent with the truth that a LHCP wave is obtained at lower band and a RHCP wave is attained at higher band.

3. PARAMETERS OPTIMIZATIONS

The mechanism of how to produce broadband radiation and circular polarization feature in the proposed antenna has been illustrated in Section 2. Some key parameters, such as the solid arc's radius r_1, the length of grounded tuning stub d and its location L_3, will be studied in this section. Their influences on the antenna's performance will be analyzed.

3.1. The Influences of r_1

Adding two arcs on the basic ring-shaped ground can not only improve the impedance matching at the lower frequency, but also help to obtain circular polarization. The influences of the dimension of r_1 on the 10 dB return loss bandwidth and the 3 dB axial ratio bandwidth are shown in Figure 8 and Figure 9. As shown in Figure 8, the investigated parameter affects the antenna's return loss and the impedance

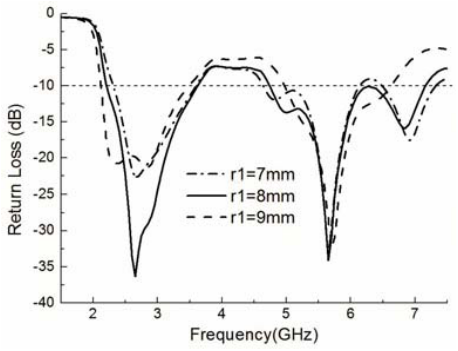

Figure 8. Return loss with different values of r_1.

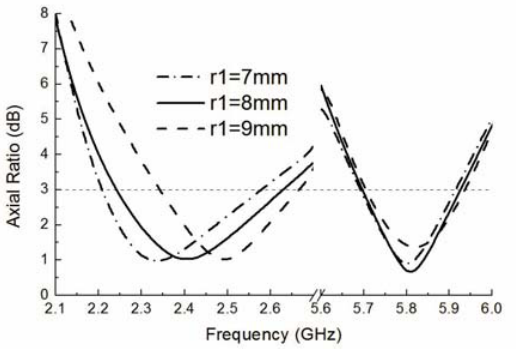

Figure 9. Axial ratio with different values of r_1.

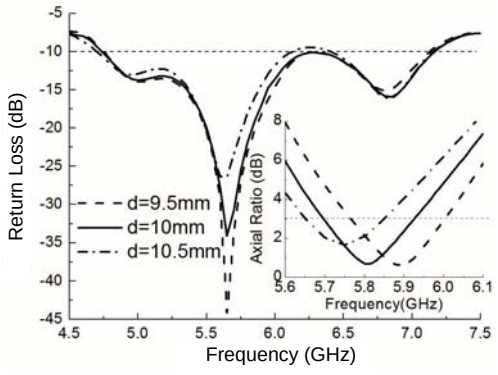

Figure 10. Return loss and axial ratio with different values of d.

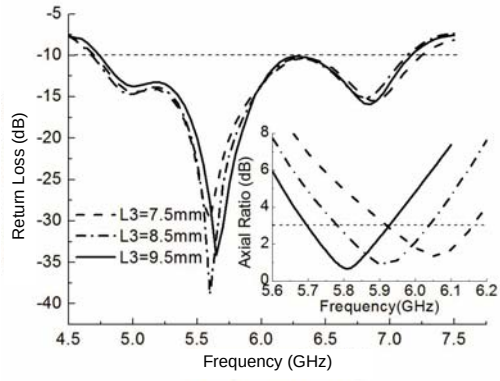

Figure 11. Return loss and axial ratio with different values of L_3.

bandwidth significantly. When it is set to be 8 mm, a better impedance matching, which includes the concerned frequencies at the lower band, is obtained. Meanwhile, a larger 10 dB impedance bandwidth at the upper band is acquired. What's more, as shown in Figure 9, the increasing dimension of r_1 leads to the corresponding AR band shifts to the higher frequencies at the lower band. But this phenomenon does not occur at the upper band, the variation just adjusts the value of antenna's AR at the interested upper frequencies. In the final design, the length of r_1 is set to be 8 mm.

3.2. The Influences of *d*

The simulated 10 dB impedance and CP bandwidth for different lengths of the grounded tuning stub d, which is located in the ring-shaped strip to adjust higher frequency CP characteristics, are presented in Figure 10. Due to its slight influences on lower band, the curves of lower frequency are not given here. As shown in this figure, when d increases a little from 9.5 mm, the impedance matching degrades rapidly. It also affects the CP resonant frequency significantly. It is noticed that the 3 dB axial ratio bandwidth moves towards lower band as d increases. In the considerations of both return loss and AR, d is set to be 10 mm, which equals to 0.19λ. Here λ is the wavelength at 5.8 GHz.

3.3. The Influences of L_3

Figure 11 shows the influences of the location (L_3) of the grounded tuning strip on the return loss and axial ratio bandwidth. Although it does not have obvious effects on the impedance bandwidth, its CP performance changes a lot for different lengths. When the location increases along the $+x$ direction, the corresponding AR will shift towards lower frequency. In this design, L_3 is set to be 9.5 mm.

4. FABRICATION AND MEASUREMENT

A prototype of the proposed antenna with optimal parameters was fabricated, as shown in Figure 12. Measurement results were obtained by using an Agilent Technology E8363B vector network analyzer (VNA) and the SATIMO measurement system.

Figure 13 shows the simulated and measured return losses of the proposed antenna. The simulated and measured results agree well. The disagreements may come from the soldering and assembling procedures, et al.. The simulated and measured 10 dB return losses are about 48.8% (2.20 GHz–3.62 GHz), 56% (2.15 GHz–3.83 GHz) at the lower band and 40.5% (4.75 GHz–7.16 GHz), 42.6% (4.67 GHz–7.2 GHz) at the upper band, respectively. The operational bands are wider than that of the designs in [23–27]. Figure 14 and Figure 15 give the comparisons of the measured and simulated radiation patterns at 2.45 GHz (the interested frequency of the lower band) and 5.8 GHz (the interested frequency of the upper band). As shown in Figure 14, overall the measured results agree well with the simulated results. The measured LHCP radiation patterns at 2.45 GHz in x-z and y-z plane are a little

Figure 12. Photograph of the proposed antenna.

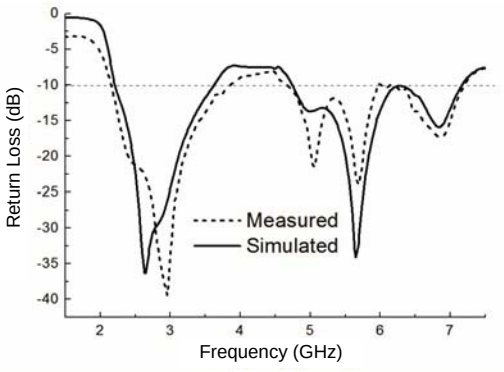

Figure 13. Measured and simulated return loss.

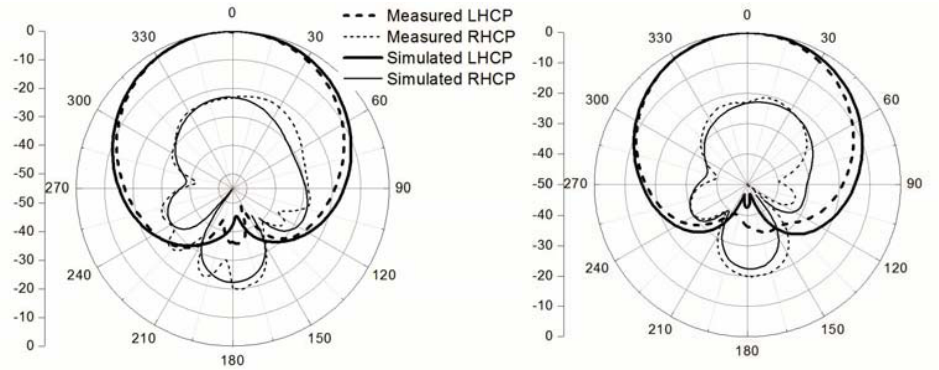

Figure 14. Measured and simulated radiation patterns, (a) x-z plane, (b) y-z plane at 2.45 GHz.

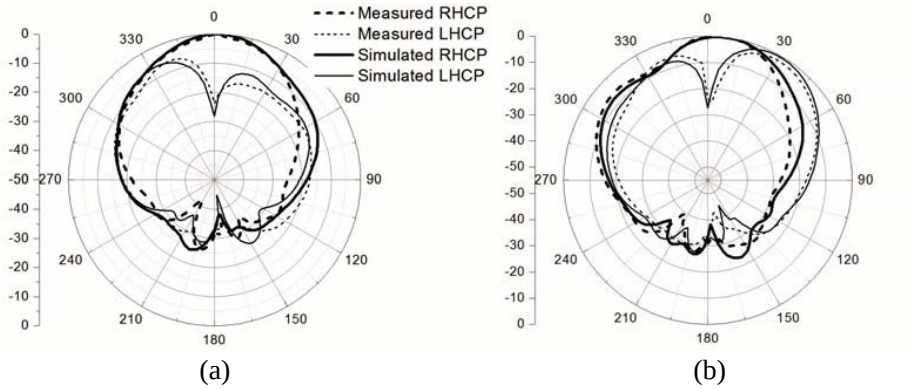

Figure 15. Measured and simulated radiation patterns, (a) x-z plane, (b) y-z plane at 5.8 GHz.

narrower than the simulated results, and the measured RHCP lobes become a little larger. Figure 15 shows that a unidirectional RHCP radiation in the $+z$ direction at the higher frequency (5.8 GHz). From the simulated and measured results, it can be concluded that the novel spherical cap reflector produces better unidirectional radiation with the great front-to-back ratio (more than 20 dB) in a large frequency ratio than the traditional plane reflector.

The measured and simulated axial ratios and gains are shown in Figure 16. Good agreements are obtained ranging from 2.24 GHz to 2.63 GHz and 5.69 GHz to 5.92 GHz. The measured 3 dB axial ratio is from 2.25 GHz to 2.62 GHz with 15.1% AR bandwidth in the lower band, and 5.67 GHz to 5.91 GHz

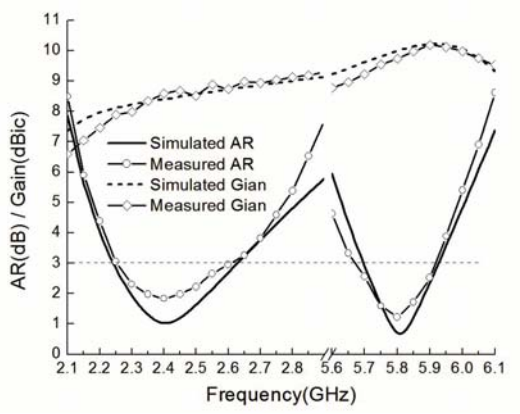

Figure 16. Axial ratio and gain of the proposed antenna.

with 4.1% AR bandwidth in the upper band. The dual operational CP bandwidths cover two wireless communication bands specified by IEEE 802.11 b/g (2.4 GHz–2.5 GHz) and IEEE 802.11 a (5.725 GHz–5.875 GHz). Figure 16 also shows the measured and simulated gains. They have same tendency with a small discrepancy. The simulated peak gain is more than 8 dBic in the two operational bands, and the maximum measured gain is as high as 8.7 dBic and 10.2 dBic respectively. The gains of the proposed antenna are lager than those dual-band unidirectional CP designs given in [23–25, 27].

5. CONCLUSION

A novel dual-band circularly polarized unidirectional antenna at 2.45 GHz and 5.8 GHz frequencies has been approached. A spherical cap reflector is used to realize the axial maximum radiation patterns in a large frequency ratio. Two wide CP bands are obtained with a F-shaped central strip, two grounded arcs and a grounded stub. From the analyses of the far field amplitude and phase difference, a LHCP wave is produced at the lower frequency, while a RHCP wave at the upper frequency. Measured results show 10 dB return loss bandwidths of 56% at 2.45 GHz and 42.6% at 5.8 GHz. Besides that, the proposed antenna exhibits a better CP behavior with the AR bandwidth of 15.1% and 4.1%, which is included in the impedance bandwidth. In addition, the maximum gain of the proposed antenna reaches to 8.7 dBic and 10.2 dBic within the two 3 dB AR bands, respectively. The presented antenna has the potential to be used for the unidirectional and high gain wireless communications.

ACKNOWLEDGMENT

This work was supported in part by the National Natural Science Foundation of China by Grants (61171044 and 61231001), the Fundamental Research Funds for the Central Universities of China (2672013ZYGX2013Z002), and the Research Fund for the Doctoral Program of Higher Education of China under Grant 20120185110024.

REFERENCES

1. Wang, P., G. Wen, J. Li, Y. Huang, L. Yang, and Q. Zhang, "Wideband circularly polarized UHF RFID reader antenna with high gain and wide axial ratio beamwidths," *Progress In Electromagnetics Research*, Vol. 129, 365–385, 2012.
2. Lee, C. H. and Y. H. Chang, "An improved design and implementation of a broadband circularly polarized antenna," *IEEE Trans. Antennas Propagat.*, Vol. 62, No. 6, 3343–3348, 2014.
3. Hu, Y. J., W. P. Ding, and W. Q. Cao, "Broadband circularly polarized microstrip antenna array using sequentially rotated technique," *IEEE Antennas and Wireless Propagat. Lett.*, Vol. 10, 1358–1361, 2011.

4. Yang, S. L. S., K. F. Lee, and A. A. Kishk, "Design and study of wideband single feed circularly polarized microstrip antennas," *Progress In Electromagnetics Research*, Vol. 80, 45–61, 2008.
5. Wu, J. W., J. Y. Ke, C. F. Jou, and C. J. Wang, "Microstrip-fed broadband circularly polarized monopole antenna," *IET Microw. Antennas Propagat.*, Vol. 4, No. 4, 518–525, 2010.
6. Rezaeieh, S. A., A. Abbosh, and M. A. Antoniades, "Compact CPW-fed planar monopole antenna with the circularly polarized bandwidth," *IEEE Antennas and Wireless Propagat. Lett.*, Vol. 12, 1295–1298, 2013.
7. Zhang, L., Y. C. Jiao, B. Chen, and Z. B. Weng, "CPW-fed broadband circularly polarized planar monopole antenna with improved ground-plane structure," *IEEE Trans. Antennas Propagat.*, Vol. 61, No. 9, 4824–4828, 2013.
8. Li, X. H., X. S. Ren, Y. Z. Yin, L. Chen, and Z. D. Wang, "A wideband twin-diamond-shaped circularly polarized patch antenna with gap-coupled feed," *Progress In Electromagnetics Research*, Vol. 139, 15–24, 2013.
9. Deng, J. Y., L. X. Guo, T. Q. Fan, Z. S. Wu, Y. J. Hu, and J. H. Yang, "Wideband circularly polarized suspended patch antenna with indented edge and gap-coupled feed," *Progress In Electromagnetics Research*, Vol. 135, 151–159, 2013.
10. Chi, L. P., S. S. Bor, S. M. Deng, C. L. Tsai, P. H. Juan, and K. W. Liu, "A wideband wide-strip dipole antenna for circularly polarized wave operations," *Progress In Electromagnetics Research*, Vol. 100, 69–82, 2010.
11. Thomas, K. G. and G. Praveen, "A novel wideband circularly polarized printed antenna," *IEEE Trans. Antennas Propagat.*, Vol. 60, No. 12, 5564–5570, 2012.
12. Wang, C. J. and C. H. Chen, "CPW-fed stair-shaped slot antennas with circularly polarization," *IEEE Trans. Antennas Propagat.*, Vol. 57, No. 8, 2483–2486, 2009.
13. Sze, J. Y., C. G. Hsu, Z. W. Chen, and C. C. Chang, "Broadband CPW-fed circularly polarized square slot antenna with lightening-shaped feedline and inverted-L ground strips," *IEEE Trans. Antennas Propagat.*, Vol. 57, No. 3, 973–977, 2010.
14. Sze, J. Y. and S. P. Pan, "Design of broadband circularly polarized square slot antenna with a compact size," *Progress In Electromagnetics Research*, Vol. 120, 513–533, 2011.
15. Jan, J. Y., C. Y. Pan, K. Y. Chiu, and H. M. Chen, "Broadband CPW-fed circularly polarized slot antenna with an open slot," *IEEE Trans. Antennas Propagat.*, Vol. 6, No. 3, 1418–1422, 2013.
16. Li, W. M., Y. C. Jiao, L. Zhou, and T. Ni, "Compact dual-band circularly polarized monopole antenna," *Journal of Electromagnetic Waves and Applications*, Vol. 25, Nos. 14–15, 2130–2137, 2011.
17. Jou, C. F., J. W. Wu, and C. J. Wang, "Novel broadband monopole antennas with dual-band circularly polarization," *IEEE Trans. Antennas Propagat.*, Vol. 54, No. 4, 1027–1034, 2009.
18. Chen, B. and F. S. Zhang, "Dual-band dual-sense circularly polarized slot antenna with an open-slot and a vertical stub," *Progress In Electromagnetics Research Letters*, Vol. 48, 51–57, 2014.
19. Chen, C. H. and E. K. N. Yang, "Dual-band circularly polarized CPW-fed slot antenna with a small frequency ratio and wide bandwidths," *IEEE Trans. Antennas Propagat.*, Vol. 59, No. 4, 1379–1384, 2011.
20. Chen, Y. Y., Y. J. Jiao, G. Zhao, F. Zhang, Z. L. Liao, and Y. Tian, "Dual-band dual-sense circularly polarized slot antenna with a C-shaped grounded strip," *IEEE Antennas and Wireless Propagat. Lett.*, Vol. 10, 915–918, 2011.
21. Weng, W. C., J. Y. Sze, and C. F. Chen, "A dual-broadband circularly polarized slot antenna for WLAN applications," *IEEE Trans. Antennas Propagat.*, Vol. 62, No. 5, 2837–2841, 2014.
22. Wu, J. N., Z. Q. Zhao, Z. P. Nie, and Q. H. Liu, "A broadband unidirectional antenna based on closely spaced loading method," *IEEE Trans. Antennas Propagat.*, Vol. 61, No. 1, 109–116, 2013.
23. Yu, A., F. Yang, and A. Elsherbeni, "A dual band circularly polarized ring antenna based on composite right and left handed metamaterials," *Progress In Electromagnetics Research*, Vol. 78, 73–81, 2008.

24. Li, Q. Q., F. S. Zhang, G. W. Zhang, B. Wang, and M. Liang, "A single-feed dual-band dual-sense circularly polarized microstrip antenna," *Progress In Electromagnetics Research C*, Vol. 51, 27–33, 2014.
25. Heidari, A. A., M. Heyrani, and M. Nakhkash, "A dual-band circularly polarized stub loaded microstrip patch antenna for GPS applications," *Progress In Electromagnetics Research*, Vol. 92, 195–208, 2009.
26. Chen, C. H. and E. K. Yung, "A novel unidirectional dual-band circularly polarized patch antenna," *IEEE Trans. Antennas Propagat.*, Vol. 59, No. 8, 3052–3057, 2011.
27. Nayeri, P., K. F. Lee, A. Elsherbeni, and F. Yang, "Dual-band circularly polarized antennas using stacked patches with asymmetric U-slots," *IEEE Antennas and Wireless Propagat. Lett.*, Vol. 10, 492–495, 2011.
28. Liu, N. W., Y. L. Yao, Z. Y. Zhang, Y. Li, G. Fu, and S. L. Zuo, "A dual-broadband circularly polarized antenna with unidirectional radiation pattern," *Progress In Electromagnetics Research C*, Vol. 51, 11–18, 2014.
29. Lu, J. H. and S. F. Wang, "Planar broadband circularly polarized antenna with square slot UHF RFID reader," *IEEE Trans. Antennas Propagat.*, Vol. 60, No. 4, 2076–2080, 2012.